A High Power High Frequency Transformer Design for Solid State Transformer Applications

Ahmad El Shafei[1], Saban Ozdemir[1,2], Necmi Altin[1,3], Garry Jean-Pierre[1], and Adel Nasiri[1]
[1]Center for Sustainable Electrical Energy Systems, University of Wisconsin Milwaukee, Milwaukee, USA
[2] Department of Electricity and Energy TBMYO, Gazi University, Ankara, Turkey
[3] Department of Electrical & Electronics Engineering, Faculty of Technology, Gazi University, Ankara, Turkey
aie@uwm.edu; ozdemir@uwm.edu; altin@uwm.edu; jeanpie4@uwm.edu; nasiri@uwm.edu

***Abstract*— In this study, design of a 330kW single-phase transformer (corresponding to 1MW three-phase) operating at 50kHz is presented. Possible core materials and their performances are investigated under high switching frequency operation. Core volume, area, configuration, and market availability are studied to achieve the optimal compact and cost-effective transformer model. Next, transformer winding type, size, placement, and cost are analyzed. These steps will result in a complete transformer electromagnetic design and modelling. Afterwards, a 3D transformer model is created and simulated using a Finite Element Analysis (FEA) tool. ANSYS Maxwell-3D is used to simulate the magnetics, electrostatics, and transients of the designed transformer. This model is integrated with a power electronics circuit in ANSYS Simplorer to make a co-simulation for the entire system. Results obtained will include core maximum flux density, core/copper losses, leakage/magnetizing inductances, windings parasitic capacitances, and input/output voltage, current, and power values. Finally, the systems' overall efficiency is calculated and presented.**

Keywords—Analysis; finite element analysis; high power; high frequency transformer; solid state transformer.

I. INTRODUCTION

Solid State Transformer (SST) has become lately one of the most popular power electronics converter types. It is a combination of a high-or medium frequency transformer and multiple power electronic converters [1]-[3]. Along with improvements in the transformer size and efficiency, it can also provide enhanced monitoring, control, and grid support functions such as providing active/reactive power as compared to Line Frequency Transformers (LFTs). Therefore, it is an attractive concept especially in renewable energy resources (RESs) integration, smart grid, and microgrid applications [4]-[6]. Studies on SSTs can be grouped basically into two distinct subjects; power converter and control design, or medium/ high frequency transformer design.

Although full-bridge PWM converters are implemented in SST applications, their switching losses limit their utilization in high power and/or medium voltage applications. Design power level can be increased by applying relatively lower switching frequency, however, this limits the decrease in transformer size and efficiency improvements of the transformer [7]-[9]. Therefore, the Phase-Shifted Full Bridge (PSFB), Series-Loaded Resonant (SLR), and Dual-Active Bridge (DAB) converters are used nowadays in SST applications [10]-[12]. These converters provide Zero-Voltage-Switching (ZVS) which increases the achievable maximum switching frequency value with a reasonable switching loss. Thus, higher efficiency and power density values are obtained.

Recently, many studies have been carried out on transformer design at different power levels and operating frequency values [13]-[20]. Based on the power level, power density, and efficiency target, the operating frequency and core material type are determined. In addition, the aforementioned power converter topologies require additional inductors for proper operation. But generally, an appropriate design of the transformer leakage inductance can eliminate this additional inductance requirement. This improves the power density, efficiency, and decreases the overall cost of the system. Therefore, and especially at high power levels, it can be seen that power converter and transformer design stages affect one another.

A 3kHz, 7kW transformer with laminated amorphous sheets core is presented in [13]. The switching frequency is low due to the limitation of the 6.5kV silicon IGBT as well as the core material characteristics. This had a direct negative impact on the transformer efficiency which was obtained to be around 91%. The revised and improved transformer design is presented in [14]. The laminated nanocrystalline core is used instead of amorphous and hence, both frequency and power levels are increased up to 20kHz and 20kW, respectively. As a result, an increase in efficiency to 96% has been achieved. In [15], a 10kHz, 35kVA nanocrystalline core transformer is designed and a 98% efficiency level is obtained. On the other hand, some work has been done on medium voltage SST as in [16]-[19]. In [16], a 37kHz, 20kW, 97% efficiency transformer is designed for 3.6kV AC grid voltage level. Also in [17], a 15kW ferrite transformer operating at 500kHz is designed for 4.16kV AC grid voltage level. This system is designed based on 3kW, 480V switching modules. The advantage of using wide-band gap switches (SiC at 800V primary side and GaN at 400V secondary side) at high frequencies and using a resonant topology, the efficiency of the system is improved to 98%. A few number of medium voltage high power SSTs are also studied. For instance, a 166kW 2kV/400V liquid cooled transformer operating at 20kHz is presented in [18]-[19]. Nanocrystalline core material is used and an improved efficiency of 99.4% is obtained. Except the latter design, all of the aforementioned studies are conducted at medium power levels.

In this study, a high power, low voltage (1kV), high frequency transformer is designed and simulated. Core material, shape, size, availability, and cost are considered as design parameters. Also, windings arrangement, leakage inductance, and parasitic capacitances are taken into account. All of these factors play a role in dictating the transformer efficiency level as well as the power transfer capability. Challenging and novel operating frequency is selected to be at 50kHz with 330kW power level to achieve high power density SST application. Different core and winding arrangements are studied in-order to maximize the coupling coefficients and hence achieve the desirable minimum leakage inductance. The complete system is simulated using ANSYS Maxwell-3D/Simplorer transient-transient co-simulation. Efficiency measured is at 98.608% level and power density is calculated to be 40.376kW/L. Thus, a highly compact and efficiency transformer design is obtained.

II. Transformer Design And Modelling

The proposed transformer specifications are given in Table I. As can be seen from the table, the transformer operates at a frequency of 50kHz with 330kW power rating which will push the conventional ratings to the limit. The two winding transformer equivalent circuit is given in Fig. 1. The leakage inductance and parasitic capacitance existing in both windings affect the transformer efficiency. In high frequency transformers, leakage inductance value must be carefully designed and chosen. It is crucial to have a small leakage inductance value in-order to transfer power to the secondary side. On the other hand, a small inductance value will cause an undesirable high *di*/*dt* rate at the switching devices. Hence, a trade should be made between these two design objectives. In such high power high frequency transformer applications, the leakage inductance value is already very high due to the number of winding layers. Hence, it is a wise decision to keep this value to a minimum. Therefore, minimizing the leakage inductance value is targeted in this study by assuming that the *di*/*dt* rate is suitable for the switches being utilized. According to this design target, the following studies have been carried out.

A. Transformer Design Formulations

Determining the transformer size and dimension is an important design milestone. This will affect a number of transformer parameters including efficiency, power density, and cost. A handy and recognized equation for determining the size of the transformer is given in (1):

$$A_P = A_C W_a = \frac{S}{K_f K_{CU} B_m f J} 10^4 \quad (1)$$

here, A_c is the core Cross-Sectional Area (CSA), W_a transformer window area, S rated apparent power, K_f applied waveform coefficient, K_{CU} window utilization factor, B_m maximum flux density, f operating switching frequency, and J current density of the conductor. According to Faraday's law, the induced voltage level of the transformer winding can be calculated as:

$$v(t) = N\frac{d\emptyset(t)}{dt} = NA_C\frac{dB(t)}{dt} \quad (2)$$

where $v(t)$ represents the induced voltage, $\emptyset(t)$ magnetic flux, and N Number of Turns (NoT). According to (2), magnetic flux density can be calculated as:

$$B_m = \frac{1}{4}\frac{E}{NA_C f} \quad (3)$$

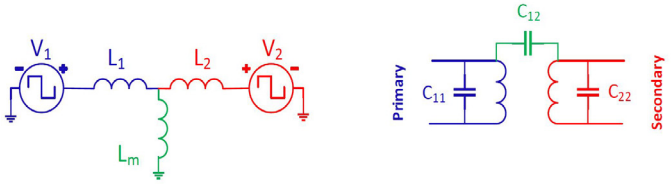

(a) (b)

Fig. 1. (a) Transformer model equivalent circuit. (b) Transformer capacitance equivalent circuit.

TABLE I. System Specifications

System Specifications	Value
Output Rated Voltage (V)	1000
Output Rated Current (A)	330
Single Phase Output Power (kW)	330
Load Resistance (Ω)	3
Switching Frequency (kHz)	50

This equation is valid for an ideal bipolar square-wave excited transformer. However, a specific dead-time interval is required during the changeover of the ON/OFF transitions of the switches. Furthermore, if the converter is designed for a specific duty cycle value, then this must also be taken into account. Thus, (3) needs some modifications according to this dead-time requirement. This is shown in (4) below:

$$B_m = \frac{1}{2}\frac{E}{NA_C}\left(\frac{T}{2} - T_d\right) \quad (4)$$

where T_d denotes the dead-time and T switching period. According to this equation, the number of turns can be found as:

$$N = \frac{E}{K_f A_C B_m f}\left(1 - \frac{T_d}{\pi}\right) \quad (5)$$

As it is well-known, a transformer has two major loss components: core and winding. For a given core material, there is a close link between these losses and the number of turns, frequency, and magnetic flux density. While increasing the number of turns can help in reducing the core losses because of the low magnetic flux density value, it increases on the other hand the winding losses. Moreover, increasing the operating switching frequency also affects the core losses. Using Steinmetz equation in (6), it is possible to calculate the core losses for a specific core material:

$$P_C = k_{ref} B^{\beta} f^{\alpha} \quad (6)$$

here, P_c is core loss while k_{ref}, α and β are core loss coefficients.

B. Core Material

Core material selection is the first and base step for transformer design. Ferrite, nanocrystalline, Si-Steel, and amorphous are the material types generally used for transformer core construction. According to [21]-[24], these types have tradeoffs and limitations at different power levels and operating switching frequencies. Table II demonstrates each material characteristics based on the high power high switching frequency application under consideration in this paper.

In-order to minimize the core power loss and keep the efficiency as high as possible, ferrite and nanocrystalline are usually used for such applications. However, nanocrystalline is

expensive compared to the ferrite core, in addition, different shapes and sizes are not available in the market as the ferrite ones. Furthermore, ferrite provides better efficiency characteristics at the desired frequency level (50kHz). Therefore, ferrite material with its abundance in the market with relatively cheap prices, high permeability, low power loss, and moderate saturation magnetic flux density (up-to 0.47T) has been chosen as the core material for this transformer design.

C. Parameters Analysis

According to the aforementioned discussion, there are many design tradeoffs and parameters that affect one another. Mainly, they are summarized by the frequency, number of turns, magnetic flux density, core and copper losses. For this purpose, MATLAB was used to develop an optimization algorithm in-order to get the optimal parameters' tradeoffs and values. Subject to the design objective, it was concluded that different core sizes and number of turns may be considered. Cost, power density, or efficiency can be selected as the primary objective design. For this transformer application, efficiency has been chosen to be the targeted and primary objective to be tackled.

Fig. 2 summarizes the variation of CSA and NoT vs. other design variables based on the system power and voltage ratings. The change in magnetic flux density (B), core losses (P_C), winding losses (P_W), and total transformer losses (P_{tr}) are presented in Fig. 2a, 2b, 2c, and 2d, respectively. Analysis of the results show that for a given system frequency range and core material, the highest efficiency is obtained when the NoT is between 11-14 and the CSA in the range of 30-36cm^2. Different U/E shapes and sizes with different ferrite characteristics available in the market have been examined. After a thorough study, using Ferrite MnZn 3C94 material from Ferroxcube with U126/91/20mm (width/height/depth) shape was concluded to be the best option for the transformer core construction in-terms of optimal cross-sectional and window areas, frequency range, flux density, and power loss [25].

III. Core Scheme Selection

Although theoretical results give an idea on the NoT and CSA, some analysis should be conducted to define the core shape, winding arrangement, and coupling style. There are three candidates defining the transformer shape: Core, Shell, and Coaxial types. Building a Coaxial type transformer at 330kW power level is not an easy or efficient option to go with. Consequently, the remaining two structures has been focused on and been compared against each other in-order to get the optimal core shape and winding arrangement.

A. Core-Type Transformer

In-order to create a Core-type transformer, using 2xU126/91/20mm results in an overall Core-type dimension of 126/182/20mm. According to Table I, the primary and secondary voltages are rated at 1kV and hence, their corresponding rated currents are around 330A. Wire cross-sectional areas higher than AWG#4 are hard to bend inside this transformer window area and wrap around its legs. Using the 500 CircularMilArea/Ampere current density industrial rule of thumb, 4xAWG#4 for primary and secondary windings is used in-order to handle the full rated current. After a mechanical and physical placement study, the optimal maximum number of

TABLE II. CORE MATERIAL CHARACTERISTICS

Core Material	Power Loss	Permeability	B_{max}	Cost	Market
Ferrite	Low	High	Moderate	Low	High
Si-Steel	High	High	High	Low	High
Nanocrystalline	Low	High	High	High	Low
Amorphous	High	High	High	Moderate	High

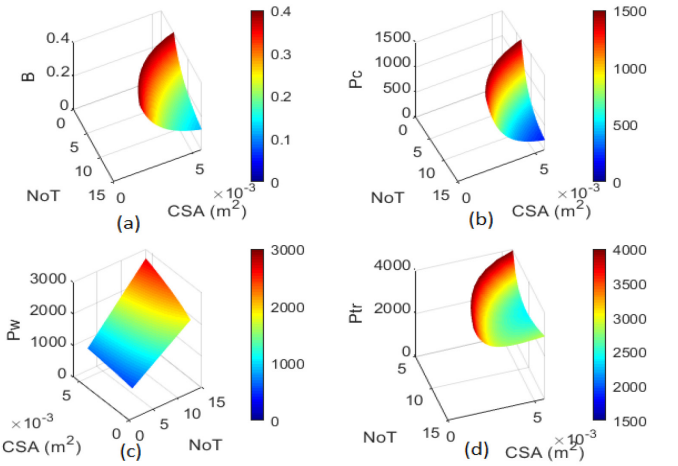

Fig. 2. Theoretical results: a) CSA vs. NoT vs. B b) CSA vs. NoT vs. P_C c) CSA vs. NoT vs. P_W d) CSA vs. NoT vs. P_{tr}

turns ended up to be 12 turns for both the primary and secondary sides. However, due to the leakage inductance and wires resistance, some voltage drop will be seen at the output. To accommodate for this drop, the number of turns for the secondary winding is chosen to be one more than that of the primary. Thus, 12 and 13 turns have been selected for the primary and secondary sides, respectively. After studying the core material saturation characteristics [26], six cascaded levels of the 126/182/20mm shape core is used to avoid core saturation giving a total of 12xU126/91/20mm shapes used. Thus, an overall transformer core size of 126/182/120mm with cross-sectional area of 33.6cm^2 and 3225.6cm^3 volume size has been obtained. Three different winding and coupling style configurations have been designed and simulated using ANSYS Maxwell-3D/Simplorer FEA tool (Fig. 3). Simulation results will be discussed in section IV.

B. Shell-Type Transformer

As discussed in the previous sections, leakage inductance is one of the most important factors determining primary to secondary power transfer limit. In addition, it affects the transformer efficiency and voltage regulation rate. The leakage inductance is highly influenced by the transformer geometric structure, shape, and number of winding layers and consequently their coupling coefficients. For instance, increasing the number of winding layers causes a corresponding increase in the leakage inductance value. In-order to reduce this high number of layers, stretching the core structure can be a remedy like a Coaxial shape transformer. However, the desired results such as energy density may not be obtained. Also, and as mentioned previously, creating this kind of core structure may not be very easy at this power and voltage levels. On the other hand, parallel and distributed winding style can be a good solution for increasing

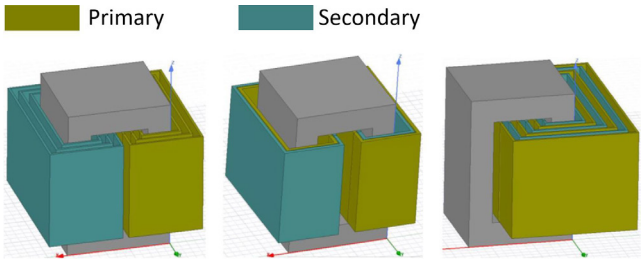

Fig. 3. Different winding configurations for the Core-type transformer.

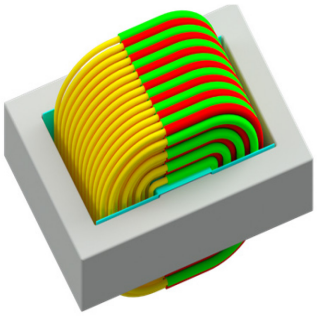

Fig. 4. Proposed Shell-type transformer 3D model.

the coupling coefficient. In this case, the voltage difference between windings should be taken into consideration for insulation reasons. Fortunately, new generation Litz wire jackets (such as Teflon) have high electrical insulation levels and they meet the partial discharge level standards.

The same Ferrite MnZn 3C94 U126/91/20mm shape and number (12xU126/91/20mm) has been used so that an exact comparison with the Core-type transformer is attained. Since the winding length and subsequently the copper losses depend on the transformer geometry, it can be seen that the Shell-type has more losses than the Core-types Type-A and Type-B. Nonetheless, it has the same windings length and losses as Type-C. For convenience, different Shell-type windings arrangement cases studied will not be presented here and only the optimal configuration will be discussed next. The proposed Shell-type transformer 3D model is given in Fig. 4. In this structure, the primary and secondary windings are wrapped together so that the coupling effect will be at its highest level and the leakage inductance at its minimum value. The core size, number of turns, core and wire cross-sectional areas are selected to be exactly the same as the previous Core-type design. That is to say, 12xU126/91/20mm resulting in a 252/182/60mm Shell-type core, 4xAWG#4 per one turn winding wire, 12/13 turns ratio, 33.6cm^2 cross-sectional area, and 3225.6cm^3 in core volume.

IV. Simulation Results

ANSYS Maxwell-3D/Simplorer FEA simulations have been carried out to study the physics, magnetics, transients, and electrostatics of the system. After modelling the transformer in Maxwell-3D, it has been imported to Simplorer in-order to simulate the entire electrical system. The Simplorer model is shown in Fig. 5. The primary winding is excited from a 1kV DC bus level high frequency inverter switching at 50kHz. Secondary winding is connected to a diode bridge rectifier which produces 1kV DC bus level for a 330kW load. This detailed transient-transient co-simulation replicates the actual physical transformer testing in real operating conditions. Next, results including core magnetic flux distribution, efficiency, transformer and load voltage/current/power will be examined.

After extracting the self/mutual inductance matrices from Maxwell-3D, the Core-type configurations leakage inductances have been calculated as 90.744µH, 1.283µH, and 2.512µH for Type-A, Type-B, and Type-C, respectively. Clearly, Type-A has a very high leakage inductance. This had a detrimental effect on the power transferred to the secondary side and thus it will be eliminated from the discussion. Type-C leakage inductance value has resulted in 11.4% voltage drop at the output and it couldn't push the full power to the secondary side. Thus, this option has been eliminated as well.

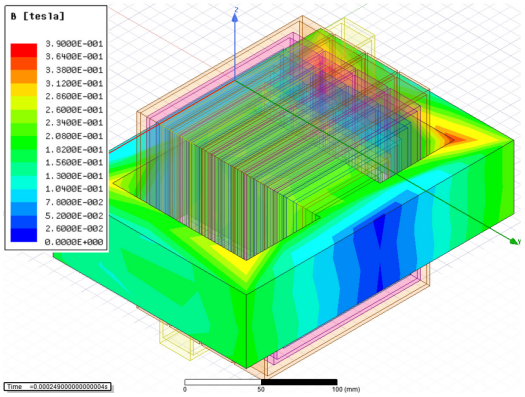

Fig. 6. Shell-type transformer flux density distribution.

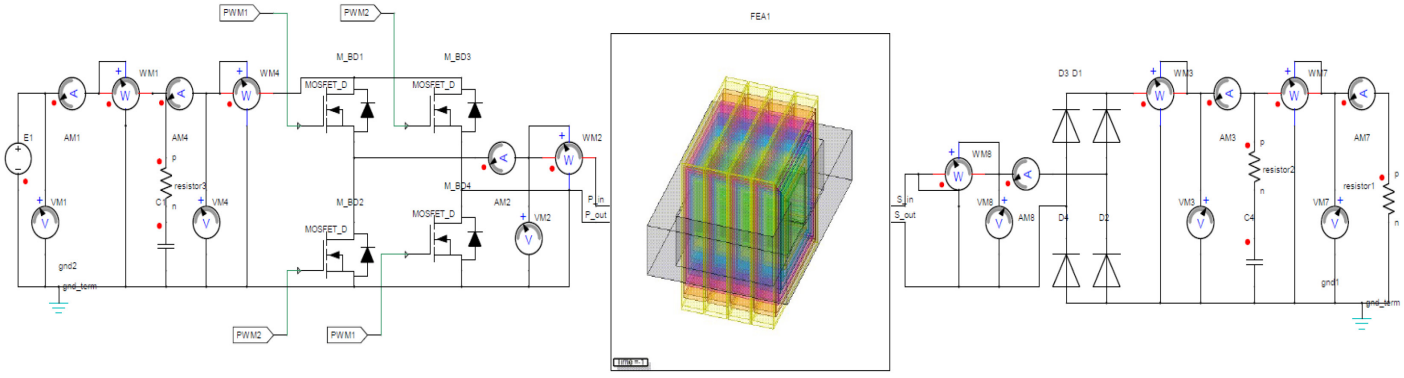

Fig. 5. The Simplorer model of the proposed converter.

TABLE III. CORE TYPE-B RESULTS

Simulation Results	Core Type-B
Maximum Flux Density, B_{max} (T)	0.288
Transformer Leakage Inductance (µH)	1.283
Magnetizing Inductance (mH)	5.877
Transformer Input Power (kW)	340.313
Transformer Output Power (kW)	322.836
Efficiency (%)	94.864

TABLE IV. SHELL TYPE RESULTS

Simulation Results	Shell-Type
Maximum Flux Density, B_{max} (T)	0.260
Transformer Leakage Inductance (µH)	1.250
Magnetizing Inductance (mH)	3.858
Transformer Input Power (kW)	338.443
Transformer Output Power (kW)	333.733
Efficiency (%)	98.608

Finally, Type-B gave good results (Table III) with small leakage inductance and only 2.25% voltage drop at the output. On the other hand, Table IV summarizes the Shell-type simulation results. Comparing results given in Table III and Table IV, the Shell-type transformer gives better results in-terms of efficiency and leakage inductance.

In Fig. 6, the proposed Shell-type transformer magnetic flux distribution is presented. As can be seen from the figure, the flux density level is around 0.2-0.3T which is the sweet spot for the ferrite MnZn 3C94 core material. Fig. 7(a) and 7(b) illustrate the Shell-type transformer voltage and current at the primary and secondary sides, respectively. The current waveform has a good and smooth shape and as expected, there is no sign of any core saturation. Moreover, the secondary voltage reached its expected rated level of 1kV. In Fig. 7(c), primary and secondary port power waveforms are presented. The average transformer input and output power levels are calculated by Simplorer and shown in Fig. 7(c) legend (WM2.P primary side, WM8.P secondary side). The transformer efficiency has been calculated to be at 98.608% level. This value is considered to be quite satisfactory for the selected power, frequency, and voltage levels. Finally, it can be seen from Fig. 7(d) that the load voltage and current waveforms reach their rated values and give the desired power level of 330kW. This figure shows also that the transformer works properly with the output rectifier and filter.

V. CONCLUSION

Nowadays, SSTs are used in medium/low power applications at high frequency, or in high power but at low frequency applications. In this study, a novel single-phase 330kW 50kHz transformer is designed and simulated. It can be utilized to build a three phase 1MW system. Since high leakage inductance value is problematic in high power high frequency applications, this paper presented a detailed study on core structure, material, winding placement, and coupling coefficients to mitigate and minimize this leakage inductance. Theoretical analysis and calculations were conducted and results were validated through FEA software tool. The designed

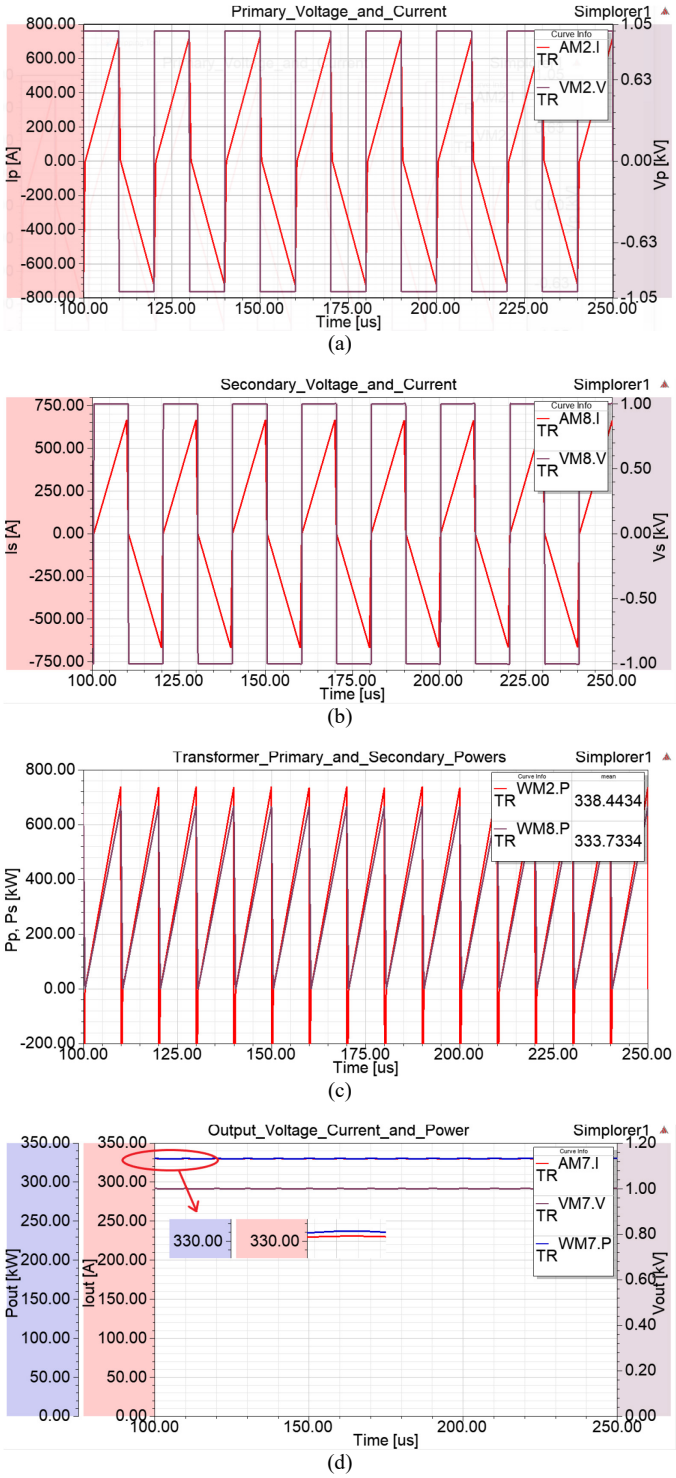

Fig. 5. Proposed Shell-type transformer results. a) Primary voltage and current b) Secondary voltage and current c) Primary and secondary power d) Load voltage and current.

transformer models were created with ANSYS Maxwell-3D and then integrated with a power electronics circuit via ANSYS Simplorer in-order to make a transient-transient co-simulation. Core-type and Shell-type transformer models have been simulated with different winding arrangements but with the same cross-sectional area, wire size, core material and size

parameters. According to the simulation results, Shell-type transformer gave better results in-terms of leakage inductance, voltage regulation, and transformer efficiency which has reached a 98.608% level. In addition, a compact design with 40.376kW/L power density is obtained.

ACKNOWLEDGMENT

This material is based upon work supported by the National Science Foundation under Grant No. 1650470. Any opinions, findings, and conclusions or recommendations expressed in this material are those of the author(s) and do not necessarily reflect the views of the National Science Foundation. Dr. Necmi Altin and Dr. Saban Ozdemir thanks the financial support which they have received from the Scientific and Technological Research Council of Turkey (TUBITAK) BIDEB-2219 Postdoctoral Research program.

REFERENCES

[1] M. Rashidi, M. Sabbah, A. Bani-Ahmed, A. Nasiri and M. H. Balali, "Design and implementation of a series resonant solid state transformer," 2017 IEEE Energy Conversion Congress and Exposition (ECCE), Cincinnati, OH, 2017, pp. 1282-1287.

[2] Kimura, Noriyuki, Toshimitsu Morizane, Isao Iyoda, Kazushige Nakao, and Tomoki Yokoyama. "Solid state transformer investigation for HVDC transmission from offshore windfarm.", 6th International Conference on Renewable Energy Research and Applications (ICRERA), pp. 574-579, 2017.

[3] Khayamy, Mehdy, Adel Nasiri, and Necmi Altin. "Development of a Power and Voltage Control Scheme for Multi-Port Solid State Transformers." 7th International Conference on Renewable Energy Research and Applications (ICRERA), pp. 926-932, 2018.

[4] S. Falcones, R. Ayyanar and X. Mao, "A DC–DC multiport-converter-based solid-state transformer integrating distributed generation and storage," IEEE Transactions on Power Electronics, vol. 28, no. 5, pp. 2192-2203, May 2013.

[5] S. Hambridge, A. Q. Huang and R. Yu, "Solid State Transformer (SST) as an energy router: Economic dispatch based energy routing strategy," 2015 IEEE Energy Conversion Congress and Exposition (ECCE), Montreal, QC, 2015, pp. 2355-2360.

[6] Rashidi, Mohammad, Abedalsalam Bani-Ahmed, Robabeh Nasiri, Azadeh Mazaheri, and Adel Nasiri. "Design and implementation of a multi winding high frequency transformer for MPSST application." 6th International Conference on Renewable Energy Research and Applications (ICRERA), pp. 491-494, 2017.

[7] M. Rashidi, A. Nasiri and R. Cuzner, "Application of multi-port solid state transformers for microgrid-based distribution systems," International Conference on Renewable Energy Research and Applications (ICRERA), Birmingham, 2016, pp. 605-610.

[8] K. Murata and F. Kurokawa, "An interleaved PFM LLC resonant converter with phase-shift compensation," IEEE Transactions on Power Electronics, vol. 31, no. 3, pp. 2264-2272, March 2016.

[9] Mohamad Sabbah, "Analysis, Design and Implementation of a Resonant Solid State Transformer," MSc. dissertation, Electrical Engineering Department, University of Wisconsin Milwaukee, Milwaukee WI, May 2016.

[10] Y. Sun and B. Jiao, "Design of a soft-switched phase-shift full bridge converter," 2016 3rd International Conference on Systems and Informatics (ICSAI), Shanghai, 2016, pp. 230-234. doi: 10.1109/ICSAI.2016.7810959

[11] N. Hinov and B. Gilev, "Modeling of Series Resonant DC-DC Power Converters," 2018 International Conference on High Technology for Sustainable Development (HiTech), Sofia, 2018, pp. 1-4. doi: 10.1109/HiTech.2018.8566410

[12] B. Feng, Y. Wang and J. Man, "A novel dual-phase-shift control strategy for dual-active-bridge DC-DC converter," IECON 2014 - 40th Annual Conference of the IEEE Industrial Electronics Society, Dallas, TX, 2014, pp. 4140-4145.

[13] G. Wang, S. Baek, J. Elliott, A. Kadavelugu, F. Wang, X. She, S. Dutta, Y. Liu, T. Zhao, W. Yao, R. Gould, S. Bhattacharca, and A. Q. Huang, "Design and hardware implementation of Gen-1 silicon based solid state transformer," in Proc. Annu. IEEE Appl. Power Electron. Conf. Expo., Mar. 6–11, 2011, pp. 1344–1349.

[14] A. Huang, X. She, X. Yu, F. Wang, and G. Wang, "Next generation power distribution system architecture: The future renewable electric energy delivery and management (FREEDM) system," Int. Conf. Smart Grids, Green Commun. IT Energy-Aware Technol., pp. 45–51, 2013.

[15] S. Balci, I. Sefa, and N. Altin. " Design and analysis of a 35 kVA medium frequency power transformer with the nanocrystalline core material," International Journal of Hydrogen Energy, vol, 42, no. 28, pp. 17895-17909, 2017.

[16] A. Huang, "Solid state transformer and FREEDM system power management strategies," NSF FREEDM Syst. Center NC State Univ., Raleigh, NC, USA, 2016. [Online]. Available: https://www.freedm.ncsu.edu/ wp-content/uploads/2016/11/FREEDM-Seminar-Series-4-Power-Manag ement-with-SSTs-by-Alex-Huang.pdf.

[17] S. Zhao, Q. Li, F. C. Lee, and B. Li, "High-Frequency Transformer Design for Modular Power Conversion from Medium-Voltage AC to 400 VDC", IEEE Transactions on Power Electronics, vol. 33, no. 9, pp. 7545-7557, September 2018.

[18] G. Ortiz, M. G. Leibl, J. E. Huber, and J. W. Kolar, "Design and experimental testing of a resonant DC–DC converter for solid-state transformers," IEEE Trans. Power Electron., vol. 32, no. 10, pp. 7534–7542, Oct. 2017.

[19] G. Ortiz, M. Leibl, J. W. Kolar, and O. Apeldoorn, "Medium frequency transformers for solid-state-transformer applications—Design and experimental verification," in Proc. IEEE 10th Int. Conf. Power Electron. Drive Syst., Apr. 2013, pp. 1285–1290.

[20] S. Ozdemir, S. Balci, N. Altin, and I. Sefa, "Design and performance analysis of the three-level isolated DC-DC converter with the nanocyrstalline core transformer", International Journal of Hydrogen Energy, vol. 42, no. 28, pp. 17801-17812, 2017.

[21] X. She, A. Q. Huang and R. Burgos, "Review of Solid-State Transformer Technologies and Their Application in Power Distribution Systems," IEEE Journal of Emerging and Selected Topics in Power Electronics, vol. 1, no. 3, pp. 186-198, Sept. 2013.

[22] Altin, N., Balci, S. Ozdemir, S. Sefa, I. "A comparison of single and three phase DC/DC converter structures for battery charging", International Conference on Renewable Energy Research and Applications (ICRERA), 2013 International Conference on, 1228 – 1233 (2013).

[23] S. Vaisambhayana, C. Dincan, C. Shuyu, A. Tripathi, T. Haonan and B. R. Karthikeya, "State of art survey for design of medium frequency high power transformer," 2016 Asian Conference on Energy, Power and Transportation Electrification (ACEPT), Singapore, 2016, pp. 1-9.

[24] S. Balci, I. Sefa, and N. Altin, "An investigation of ferrite and nanocrystalline core materials for medium-frequency power transformers", Journal of Electronic Materials, vol. 45, no. 8, pp. 3811-3821, 2016.

[25] Designed by Akacia System, www.akacia.com.tw, "Cores & Accessories," Ferroxcube. [Online].Available: https://www.ferroxcube.com/en- global/products_ ferroxcube/stepTwo/ shape_cores_accessories?s_sel=161&series_sel=&material_sel=3C94& material=&part=.[Accessed: 21-Aug-2019].

[26] Designed by Akacia System, www.akacia.com.tw, "Power Conversion," Ferroxcube. [Online]. Available:https://www.ferroxcube.com/en-global/ak_material/index/power_conversion. [Accessed: 21-Aug-2019].